Published in final edited form as:
DNA Repair (Amst). 2013 November ; 12(11): . doi:10.1016/j.dnarep.2013.08.008.

Dynamics of Enzymatic Interactions During Short Flap Human Okazaki Fragment Processing by Two forms of Human DNA Polymerase δ

Szu Hua Sharon Lin, **Xiaoxiao Wang**, **Sufang Zhang**, **Zhongtao Zhang**, **Ernest Y.C. Lee**, and **Marietta Y.W.T. Lee***
Department of Biochemistry and Molecular Biology, New York Medical College, Valhalla, NY 10595

Abstract

Lagging strand DNA replication requires the concerted actions of DNA polymerase δ, Fen1 and DNA ligase I for the removal of the RNA/DNA primers before ligation of Okazaki fragments. To better understand this process in human cells, we have reconstituted Okazaki fragment processing by the short flap pathway *in vitro* with purified human proteins and oligonucleotide substrates. We systematically characterized the key events in Okazaki fragment processing: the strand displacement, Pol δ/Fen1 combined reactions for removal of the RNA/DNA primer, and the complete reaction with DNA ligase I. Two forms of human DNA polymerase δ were studied: Pol δ4 and Pol δ3, which represent the heterotetramer and the heterotrimer lacking the p12 subunit, respectively. Pol δ3 exhibits very limited strand displacement activity in contrast to Pol δ4, and stalls on encounter with a 5'-blocking oligonucleotide. Pol δ4 and Pol δ3 exhibit different characteristics in the Pol δ/Fen1 reactions. While Pol δ3 produces predominantly 1 and 2 nt cleavage products irrespective of Fen1 concentrations, Pol δ4 produces cleavage fragments of 1–10 nts at low Fen1 concentrations. Pol δ3 and Pol δ4 exhibit comparable formation of ligated products in the complete system. While both are capable of Okazaki fragment processing *in vitro*, Pol δ3 exhibits ideal characteristics for a role in Okazaki fragment processing. Pol δ3 readily idles and in combination with Fen1 produces primarily 1 nt cleavage products, so that nick translation predominates in the removal of the blocking strand, avoiding the production of longer flaps that require additional processing. These studies represent the first analysis of the two forms of human Pol δ in Okazaki fragment processing. The findings provide evidence for the novel concept that Pol δ3 has a role in lagging strand synthesis, and that both forms of Pol δ may participate in DNA replication in higher eukaryotic cells.

Keywords

DNA polymerase δ; DNA replication; Okazaki fragment; lagging strand; Fen1, flap endonuclease 1

*To whom correspondence should be addressed. Marietta Lee, Department of Biochemistry and Molecular Biology, New York Medical College, Valhalla, NY 10595. marietta_lee@NYMC.edu. Tel: 1-914-594-4070.

Conflict of interest
The authors declare that they have no conflict of interest.

1. INTRODUCTION

The process of DNA replication at the replication fork requires that the two daughter strands be coordinately synthesized. Because of the different polarity of the DNA strands, the leading strand is continuously extended in the 5' to 3' direction, while the lagging strand is discontinuously synthesized by the production and joining of Okazaki fragments. The length of Okazaki fragments differs from prokaryotes to eukaryotes. In eukaryotes, the Okazaki fragments are only about 200 nt in length. The synthesis of eukaryotic Okazaki fragments starts with the generation of RNA/DNA primers (8–12 RNA nts followed by 10–20 DNA nts) by Pol α/primase, which are extended by the replicative proofreading DNA polymerases. These primers must be removed before ligation of the Okazaki fragment to the lagging strand, because of their RNA content and also because Pol α does not possess a proofreading 3' to 5' exonuclease and is error prone. Thus, the process requires the removal of the RNA/DNA primer when it is encountered by a new Okazaki fragment and the formation of a nick (reviewed in [1–3]) that can be sealed by DNA ligase I [4,5]).

The 5' ends of Okazaki fragments include DNA synthesized by Pol α (which is less accurate than Pol δ as it lacks a proof reading 3' to 5' exonuclease) which are likely to contain errors. Thus, the removal of these ends during Okazaki fragment processing can be considered in the broader perspective of a replication-coupled DNA repair process. In addition, the processes of gap filling in DNA repair processes such as during nucleotide excision repair also bears resemblances to Pol δ/Fen1 reactions. Thus, both Fen1 and Pol δ are recruited to sites of nucleotide excision repair with similar kinetics in *in vitro* assays [6], while Fen1 also plays a role in base excision and mismatch repair [7–9].

The major pathway for the removal of the RNA/DNA primer is the short flap pathway. This pathway involves limited strand displacement by Pol δ, which creates short flaps (1–8 nts) that are cleavable by flap endonuclease 1 (Fen1) [10]. Longer flaps are poor substrates for Fen1, and these are removed by intervention of a long flap pathway [1,10,11]. Flaps longer than *ca*. 25 nts are bound by RPA and cleaved by Dna2 nuclease/helicase, leaving a shorter flap that is processed by Fen1. A helicase, Pif1, also cooperates to extend longer flaps and to unwind fold-back flap structures [12,13]. The short flap pathway has been extensively studied in yeast by both biochemical and genetic analyses [14–16]. These studies illuminated several key properties of yeast Pol δ which reveal adaptations that are suited for its role in Okazaki fragment processing. Yeast Pol δ has been shown to perform limited strand displacement under certain conditions, and idles, leading to the maintenance of a nick suitable for ligation under the conditions used in reconstituted systems [17,18]. These properties are not shared by yeast Pol ε [16,17], consistent with the concept of a division of labor between yeast Pol δ and yeast Pol ε at the lagging and leading strands, respectively [1,19,20]. In addition, Pol ε has been shown to be organized in the replisome complex through association with the CMG helicase (Cdc45, Mcm2–7, and GINS) [21–23], supporting its role as a leading strand polymerase.

The shuttling of the enzymes responsible for the primer extension, removal of primer sequences and subsequent ligation is coordinated by the processivity factor PCNA, which is a trivalent molecule that can accommodate multiple protein partners through its affinity for PIP-box containing proteins [24]. All three components of the Okazaki processing system, (Pol δ, Fen1 and DNA ligase I) are PCNA binding proteins. The role of PCNA as a platform that co-ordinates and synchronizes the reactions in Okazaki fragment has been greatly advanced by studies of the archaeon, *Sulfolobus solfataricus*, where structural evidence has led to a model in which the polymerase (PolB1), Fen1 and DNA ligase reside on archaeal PCNA to form a complex [25–28]. Whether this model is conserved in eukaryotes is still incompletely defined.

The details of the biochemistry and functions of the combined Pol δ/Fen1 reactions of the short flap pathway in the human or higher eukaryotes have not been as intensively studied as in yeast, although the functions of human Fen1 and Dna2 have been well characterized [2,3,18]. Human Pol δ (Pol δ4) is a heterotetramer composed of the p125 catalytic subunit, p50, p68 and p12 subunits [29–32]. Studies of human Pol δ have been facilitated by the reconstitution of recombinant Pol δ4 and its subassemblies by their expression in Sf9 cells [33,34]. Pol δ4 has multiple interactions with PCNA, since p125, p68 and p12 bind to PCNA (reviewed in [32]). The Pol δ trimer lacking the p12 subunit (Pol δ3) is of particular interest, since it is generated *in vivo* by the targeting of the p12 subunit is targeted for degradation in response to UV and alkylating agents as well as replication stress [32,35]. Analysis of the subcellular localization of Pol δ subunits in response to UV indicates that Pol δ3 is present at sites of DNA damage long before repair is complete, so that Pol δ3 is the form of Pol δ activity that is likely involved in gap filling reactions during DNA repair. Biochemical analyses of the properties of Pol δ4 and Pol δ3 in bypass synthesis across template lesions revealed properties that are consistent with the idea that its presence might be of benefit when cells are subjected to genotoxic challenges. Pol δ3 exhibited a reduced tendency for lesion bypass, and stalled more readily on encounter with template lesions. In addition, it exhibited signs of greater proofreading and discrimination against incorporation or extension of mismatched primer ends [36,37]. Thus, the p12 subunit modulates the key kinetic parameters of human Pol δ that determine its behavior on encounter with template lesions and its proofreading abilities. Human Pol δ differs from its counterpart in *S. cerevisiae*, as yeast Pol δ lacks the p12 subunit [38]. Analyses of p12 levels in synchronized cell populations and laser scanning cytometric analysis indicated that p12 levels, unlike those of the other subunits, are reduced in S phase [39,40]. This evidence that Pol δ3 is formed in S phase during normal cell cycle progression suggests that it participates in DNA replication [39,40].

In this study, we have examined the behavior of Pol δ4 and Pol δ3 in the reactions which are required for Okazaki fragment processing in cooperation with Fen1, as well as in the complete reconstituted system that included DNA ligase I. Our studies reveal that while Pol δ4 is competent in cooperating with Fen1 in the generation and removal of short flaps, Pol δ3 exhibits near-ideal characteristics for participation in Okazaki fragment processing. In addition, the comparative analysis of Pol δ3 and Pol δ4 provides insights into the role of strand displacement behavior in the determination of cleavage product size distribution.

2. MATERIALS AND METHODS

2.1 Proteins for the reconstitution of Okazaki fragment processing

Recombinant human Pol δ4 and Pol δ3 were expressed in Sf9 cells and purified to near-homogeneity by reproducible procedures that included immunoaffinity chromatography using immobilized anti-p125 [34]. Their specific activities were determined by standard assays on poly(dA)/oligo(dT) and conformed to those reported previously [34]. All the Pol δ subunits were untagged. Protein concentrations were based on the amounts of the p125 subunit as determined by SDS-PAGE and Coomassie blue staining with different concentrations of a standard protein (catalase) [34]. The human Fen1 coding sequence was cloned into the pET-41b(+) expression vector (Novogen) between the NdeI and XhoI sites to generate fusion proteins with a C terminal six histidine-tag. Recombinant Fen1 was purified on Ni-NTA-agarose (QIAGEN) with the protocol recommended by the manufacturer. Fen1 was then stored at −80°C after addition of 10% glycerol. pFastBacHTb-ligase I was generated by PCR using pCMV6-XL5-ligase I (Origene) as the template. Baculovirus for the expression of human DNA ligase was generated using the Bac-to-Bac system (Invitrogen) and used to infect Sf9 cells. DNA ligase I was purified by metal chelating chromatography. Human PCNA was expressed in *E. coli* and purified to homogeneity as

described previously [41]. The concentrations of human Fen1, PCNA and DNA ligase I were determined by SDS-PAGE and Coomassie blue staining with a standard curve of increasing amount of catalase protein. RFC (Replication factor C) was used as described previously [42].

2.2. Oligonucleotide Substrates

All oligonucleotides were purchased from Integrated DNA Technologies and purified by PAGE before use. The sequence of each oligonucleotide is listed in Supplemental Table A1. The substrate was either 5'- labeled or 3'-labeled. The 5' end labeling reaction was conducted at 37°C for 1 h in a 30 μl reaction containing 150 pmole of the target DNA, 70 mM Tris-HCl buffer pH 7.6, 10 mM $MgCl_2$, 5 mM DTT, 15U T4 polynucleotide kinase (NEB) and [γ-^{32}P]ATP (MP Biochemicals). The labeled dsDNA was purified with a QIAquick Nucleotide Removal Kit (QIAGEN). A target DNA was annealed to a template with a single nt 5'-overhang prior to 3'-end labeling. The 3'-end labeling reaction was conducted at 37°C for 2 h in a 30 μl reaction containing 200 pmole of the dsDNA from the annealing sample, 10 mM Tris-HCl buffer pH 7.9, 50 mM NaCl, 10 mM $MgCl_2$, 1 mM DTT, 10U Klenow fragment 3' '5' exo$^-$ (NEB) and [α-^{32}P]dNTP (MP Biochemicals). The labeled dsDNA was purified with a QIAquick Nucleotide Removal Kit (QIAGEN). A selected template and a 5'-blocking oligonucleotide were annealed to the labeled DNA. The annealing procedure was conducted at 95°C for 5 min followed by 65°C for 20 min. The annealed substrate was stored at −20°C.

2.3. Reconstitution assays

DNA polymerase activity, Fen1 cleavage and nick ligation reactions were analyzed by sequencing gels. A standard protocol consisted of a 10 μl solution containing 50 mM Tris-HCl pH 7.5, 1 mg/ml BSA, 125 mM NaCl, 5 mM DTT, 0.5 mM ATP, 5 mM $MgCl_2$, 100 μM dNTP and the selected oligonucleotide substrate unless otherwise indicated. Reaction was either initiated by $MgCl_2$ or by addition of the enzymes. The reaction was allowed to proceed for defined times at 37°C and then quenched by addition of 5 μl stopping solution (0.02% bromophenol blue, 0.02% Xylene cyanol, 50 mM EDTA, 90% formamide). The resulting samples were heated at 95°C for 5 min and placed on ice immediately. The products of DNA synthesis, Fen1 cleavage and nick ligation were analyzed by sequencing gels (composed of 16~20% acrylamide/bisacrylamide 19:1 (Bio-Rad), 7.4 M Urea, 1 mM EDTA, 90 mM Tris-HCl and 90 mM boric acid). Reaction products were visualized by phosphorimaging Molecular Dynamics Storm Phosphorimaging system and quantified with ImageQuant (Amersham Biosciences). All experiments were repeated at least three times, and data for representative experiments are shown.

3. RESULTS AND DISCUSSION

3.1 Overall experimental approach

Recombinant human proteins (Pol δ4, Pol δ3, Fen1, DNA ligase I and PCNA) purified to near homogeneity were used in these studies (Materials and Methods). The stoichiometry of the subunits of Pol δ4 and Pol δ3 were examined by SDS-PAGE, and were close to the expected one to one ratios. This confirmed that p12 was stoichiometrically present with the other Pol δ subunits in Pol δ4, and absent in Pol δ3 preparations. All of the Pol δ subunits were untagged. For the overall experimental strategy we first examined the strand displacement activities of Pol δ4 and Pol δ3, followed by the combined reactions of Pol δ4 and Pol δ3 with Fen1, and finally the complete system with DNA ligase I. Conditions were chosen which reflected near-physiological ionic strength and optimized the requirements of both Pol δ and Fen1. The substrates used to examine Okazaki fragment processing (removal of the 5'-end of the prior Okazaki fragment by the concerted Pol δ/Fen1 reactions and

subsequent ligation) were oligonucleotides in which a primer and a 5'-blocking oligonucleotide were annealed to a template (see below). For most of our studies we used biotinylated templates which were capped with streptavidin, similar to those used in the previous studies of the yeast system [14,15].

3.2. Pol δ4 strand displacement of DNA and RNA 5'-blocking oligonucleotides

The substrates used for analysis of the strand displacement activities of Pol δ4 consisted of a 107mer template to which a 5'-[^{32}P]labeled 30mer was annealed, followed by a gap of 30 nts and a 5'-blocking oligonucleotide annealed to positions 61–77 of the template [14,15]. Three different 5'-blocking oligonucleotides were used in this experiment, a 16mer DNA oligonucleotide (D_{16}), a 16mer DNA preceded by a 10 nt flap formed by noncomplementary nucleotides ($F_{10}D_{16}$), and a 17mer consisting of 9 RNA nucleotides followed by 8 DNA nucleotides (R_9D_8) (Fig. 1A). In the presence of Pol δ (10 nM), gap-filling is initiated, so that the encounter with the 5'-blocking oligonucleotide is a dynamic one. A 60mer is formed after gap-filling, and further extension of the labeled primer represents strand displacement until the end of the template is reached to form a 77mer (Fig. 1A).

Pol δ4 readily performs strand displacement synthesis on all three substrates (Fig. 1B). Pol δ4 initially stalls at the nick position, *i.e.*, just before the annealed 5'-blocking oligonucleotide, as shown by the accumulation of the 60mer, but readily continues synthesis after encountering the block. The amounts of the 60mer and 77mer products were quantitated by phosphorimaging, and plotted against time (Fig. 1C). Similar amounts of 60mer and 77mer products were produced when DNA 5'-blocking oligonucleotides with ($F_{10}D_{16}$), or without a flap (D_{16}) were used. On the other hand, the RNA/DNA hybrid 5'-blocking oligonucleotides (R_9D_8) resulted in more significant stalling as demonstrated by a decreased 77mer/60mer ratio (Fig. 1C), where the accumulation of the 60mer exceeded that of the 77mer. This latter result indicates that a RNA 5-blocking oligonucleotide poses a significantly greater impediment than a DNA sequence to strand displacement by Pol δ4, with a *ca*. 3–4 fold lower rate of accumulation of the 77mer strand displacement product. This behavior might be of significance in a cellular context, given that the strand displacement activity of Pol δ4 would be reduced on encounter with the RNA end. We also compared strand displacement of Pol δ4 on the R_9D_8 substrate, and a substrate identical to $F_{10}D_{16}$ except that the flap was 2 nts long. This gave similar results (data not shown).

3.3. Comparison of the strand displacement activities of Pol δ4 and Pol δ3 reveals that Pol δ3 exhibits little strand displacement activity

The template/primer designs used for the comparison of the strand displacement activities of Pol δ4 and Pol δ3 consisted of a 70mer template end labeled with biotin, annealed to a 5'-[^{32}P]end labeled primer, with a 5 nt gap before the blocking oligonucleotide. These were capped with streptavidin to prevent PCNA from sliding off the DNA [14,15]. Such substrate designs require the loading of PCNA with RFC. The substrates used were a 31mer, D_{31} (Fig. 2A), and a 31mer with a 4 nt flap, F_4D_{31} (Fig. 2B). Pol δ4 (20 nM) exhibited very little stalling after gap filling to form the 39mer, and exhibited robust strand displacement activity to generate the full-length 70mer with both substrates (Fig. 2C, left panel). The results are consistent with the observations made with the uncapped substrates used in Fig. 1, except that the strand displacement reactions were more efficient with the capped substrates. The behavior of Pol δ4 is similar to that observed with the trimeric yeast Pol δ [14–17].

Pol δ3 exhibited a striking difference from the behavior of Pol δ4 (Fig. 2C, right panel). Almost negligible amounts of the 70mer were formed, showing the near-absence of strand displacement activity. Similar results were obtained when the Pol δ3 concentration was increased 4-fold to 80 nM (data not shown). With both the fully annealed (D_{31}) and the 4 nt

flap (F_4D_{31}) 5'-blocking oligonucleotides, Pol δ3 was stalled after gap filling to form the 39mer. Small amounts of 40mer representing the addition of a single nt were formed. Quantitation of the amounts of 70mer formed by Pol δ4 and Pol δ3 with both substrates is shown in Fig. 2D. The rates of strand displacement were estimated by graphical analysis of the linear portions of the time courses. The ratios of the strand displacement rates of Pol δ4 to Pol δ3 were 11:1 and 19:1 for the D_{31} (no flap) and the F_4D_{31} (4nt flap) substrates, respectively.

It was noticed that in the presence of the 4nt flap, the nick was not maintained at the 39nt position and there was the appearance of smaller 36mer to 38mer products (Fig. 2C, right panel). The likely explanation as to why this only occurs when the flap is present is that the presence of the flap acts as a steric hindrance to the polymerase reaction, so that resynthesis during the idling process is impeded.

Thus, Pol δ3 performs very limited strand displacement, and stalls on encounter with the 5'-blocking oligonucleotides with or without a flap. Such stalling reactions are not passive, but represent an active process in which short extension of the primer is followed by exonucleolytic cleavage in what has been termed an idling process as shown by extensive studies of yeast Pol δ [14–17]. The iterative process of strand displacement and exonucleolytic cleavage avoids the formation of a gap to maintain of a nick that can be ligated [16]. The behavior of Pol δ3 which is observed here is remarkably similar to that displayed when it encounters template lesions where it exhibits greater stalling behavior than Pol δ4. In fact, the pattern of products formed by Pol δ3 (Fig. 2C, right panel) resembles that exhibited on templates containing an AP site [36]. The mechanistic basis for the increased stalling and exonucleolytic behavior of replicative DNA polymerases with proofreading 3' to 5' exonuclease activities at template lesions is well understood [43–45]. Our previous studies using pre-steady state kinetic analysis of Pol δ3 and Pol δ4 have revealed the mechanisms for the increased proofreading by Pol δ3; its kinetic constants for the polymerization step, k_{pol}, for Pol δ3 is decreased, and that for the translocation of the primer end from the polymerase to the exonuclease active site, $k_{pol\text{-}exo}$, is increased [37]. These two kinetic constants govern the proofreading abilities of replicative polymerases [43,45]. The differences in these properties between Pol δ4 and Pol δ3 that provide a mechanistic explanation for the greater stalling at template lesions by Pol δ3 is also applicable to its behavior in strand displacement. The overt level of strand displacement by Pol δ3 is largely limited to a single nucleotide, which could be interpreted as due to fraying of the 5' end of the blocking oligonucleotide.

The striking difference in strand displacement exhibited by Pol δ4 and Pol δ3 are relevant to considering their functions in DNA repair. The gap filling reactions in DNA repair, as during nucleotide excision repair or base excision repair, bear some similarities to the reactions in Okazaki fragment processing. The attributes of Pol δ3 are more appropriate for a role in gap filling than Pol δ4, since it avoids excessive strand displacement. Pol δ4 has been shown to be able to perform D-loop extension during homologous recombination [46]. However, in homologous recombination reactions, extension of the invading strand does require the ability for strand displacement. In this context, it would be predicted that Pol δ4 would be far more effective than Pol δ3 in the extension of the invading strand in the D-loop during homologous recombination.

3.4. Combined Pol δ strand displacement-Fen1 cleavage reactions

In order to characterize the nature of the products formed by the concerted action of Pol δ and Fen1 we used a substrate similar to that used in Fig. 2A in which the labeled primer was followed by a 15 nt gap and a 5'-blocking 20mer (Fig. 3A). The time course of the reactions was followed over a period of 80 seconds to observe the early stages of the reactions. Pol δ4

(50 nM) alone readily performed strand displacement, as shown by formation of the 70mer, with very little stalling as indicated by accumulation of a 49mer (Fig. 3B, first panel). When Fen1 (100 nM) was present, the pattern of product formation was altered, with a reduction of the 70mer, and the appearance of intermediate products starting from the 49mer (Fig. 3B, second panel). A similar effect was seen with Pol δ3, which produced more products in the 49mer range because of stalling (Fig. 3B, third panel), but produced a range of intermediate products was produced between the 49 – 70 nt range in the presence of Fen1 (Fig. 3B, fourth panel). These represent the elongation of the primer, as the 5'-blocking oligonucleotide is progressively shortened by Fen1 cleavage.

Next we used a nicked substrate (Nick-D_{35}) in which the gap was removed, so that a longer 5'-blocking oligonucleotide was present (Fig. 3C). The longer blocking sequence allowed a better resolution of the intermediate products on the gels. Pol δ4 alone exhibited a robust strand displacement reaction (Fig. 3D, first panel) as evidenced by formation of the 70mer, with few intermediate products. In the presence of Fen1, the intermediate products are more prominent, and the appearance of a ladder is now clearly visible (Fig. 3D, second panel). The amounts of 70mer formed in the presence of Fen1 was also decreased, offset by the formation of the intermediate products. Thus, the strand displacement reaction is converted to the coupled reaction of primer extension/Fen1 cleavage of the 5'-blocking oligonucleotide.

With Pol δ3 alone, only limited strand displacement is observed, with accumulation of the 35mer representing the primer+1 product, and very little 70mer (Fig. 3D, third panel). In the presence of Fen1, primer extension takes place and the formation of a ladder is now distinct (Fig. 3D, fourth panel). These results indicate that the apparent inability of Pol δ3 for strand displacement does not prevent it from participating in the coupled Fen1 reaction, *i.e.*, Fen1 now enables primer extension by Pol δ3 as it cleaves the 5'-blocking oligonucleotide. No major accumulation of the 70mer is evident, so that the intermediate products formed can be attributed to the combined actions of Pol δ3 and Fen1. The formation of the ladder (Fig. 3D, fourth panel) is significant since it is consistent with the observation that mononucleotides are the primary products being cleaved by Fen1 in concert with Pol δ3 or Pol δ4 in the first cleavage reaction (see below).

The results of the preceding experiments (Figs. 2 and 3) provide a view of the combined reactions of human Pol δ3 and Pol δ4 with Fen1 that take place in the removal of the 5'-ends of Okazaki fragments. These are shown diagrammatically to allow a qualitative interpretation of the nature of the products observed (Figs. 3E, F). The strand displacement behavior for Pol δ4 shows that it progresses through the formation of a flap that is steadily displaced, so that the full length product accumulates with very few intermediate products (Fig. 3E). The flap size continuously increases, so that the rate of strand displacement probably does not change significantly. When both Pol δ and Fen1 are present, a repetitive process takes place, in which Pol δ introduces a flap by limited strand displacement, and is switched with Fen1 which cleaves the flap (Fig. 3F). The process results in the progressive exonucleolytic degradation of the 5'-blocking oligonucleotides, and the stepwise elongation of the primer (Fig. 3F). This is observed in Figs. 3C and D, which shows a ladder of labeled products of increasing size which is evident for both Pol δ4 and Pol δ3.

3.5. Kinetic analysis of the flap cleavage products formed by the concerted actions of Pol δ4/Fen1 and Pol δ3/Fen1

The purpose of these experiments was to determine the rate of the formation of cleavage products as well as their size distribution when Pol δ4 or Pol δ3 acts in combination with Fen1. In order to analyze the flap cleavage products, we used the Gap-D_{20} substrate in which the 5' end of the 5'-blocking 20mer was labeled. With this substrate the cleavage

fragments are generated in a dynamic system where the gap provides a “running start” for Pol δ. In this arrangement, the labeled products represent the first cleavage of the 5’-blocking oligonucleotide, as subsequent cleavages yield unlabeled products (Fig. 4A). At the encounter of the moving Pol δ/PCNA complex with the 5’ end of the blocking oligonucleotide, Pol δ would be initially stalled and then begin strand displacement, forming flaps which are then cleaved by Fen1. This results in the generation of labeled fragments which represent the spectrum of the first cleavage products by Fen1. The data shown are representative of multiple experiments that were performed.

The time course of the combined Pol δ4/Fen1 and Pol δ3/Fen1 was examined at different Fen1 concentrations (5, 10, 20, 50 nM) with 20 nM Pol δ4 or Pol δ3 and analyzed by gel electrophoresis. Phosphorimages of the gels for the 10 and 50 nM Fen1 concentrations are shown as examples for Pol δ4 (Fig. 4B) and Pol δ3 (Fig. 4C). With Pol δ4, the products formed at 10 nM Fen1 were distributed mainly between 1 – 8 nts, and this was shifted to a shorter product range with a predominance of 1 nt products at 50 nM Fen1. In the case of Pol δ3, the product range was lower, with mononucleotides being predominant, and similar patterns at both Fen1 concentrations. The data for the entire series was quantitated, and the amounts of each cleavage product from 1 to 10 nts were determined. These were then summed up for each time point in order to determine the total product formation at each Fen1 concentration (Fig. 4D, 4E). With Pol δ4, the combined reaction was slower at 5 nM Fen1 but exhibited only small increases at the 10–50 nM Fen1 concentrations, and reached maximum conversion at about 70%. This is consistent with the strand displacement step being the rate limiting step of the combined reaction. With Pol δ3 (Fig. 4E), the rates of product formation were similar at the three lower Fen1 concentrations, with a slight increase at 50 nM Fen1. Maximal product formation was slightly lower than for Pol δ4, at 50–60%.

Next, we analyzed the rates of formation for each of the cleavage fragment sizes from 1 – 8 nts for Pol δ4 at the different Fen1 concentrations (Fig. 5). At 5 nM Fen1, the products were roughly distributed between all fragment sizes, with the 4 and 5 nt fragments being predominant. With increasing Fen1, the cleavage product size progressively shifted to shorter products, such that at 50 nM Fen1 the predominant cleavage product was 1 nt, with smaller amounts of the 2 3 and 4 nt products, and very little of the products >5 nts. This effect on cleavage fragment size with increasing Fen1 can be explained by the rate limiting nature of the strand displacement reaction, since the rate of formation of each flap is directly related to the number of polymerization steps needed.

The product size distribution when Pol δ3 and Fen1 were used revealed a very different picture, in that there was great similarity in the rates of product formation and the product size distribution (Fig. 6). The 1 and 2 nt cleavage products were the predominant ones, with lesser amounts of the 3 and 4 nt products, and products > 5 nt were barely above background; only at 50 nM was there a marked difference, in that formation of the 1 nt product was increased (Fig. 6D). Similar considerations of the strand displacement being the rate-limiting factor as with Pol δ4 can be made. The rates of formation of the 1 and 2 nt products are almost identical at the three lower Fen1 concentrations (Fig. 6A, 6B, 6C), providing a clear indication that Pol δ3 strand displacement is limiting. Another factor could be that Pol δ3 exhibits little tendency for strand displacement, and in fact only presents the 1 or 2 nts flaps for Fen1 to act upon. Thus, in both the case of Pol δ4 and Pol δ3, flap cleavage is constrained to short flaps, and in the case of Pol δ3, is at the extreme where the predominant reaction is a nick translation reaction which is limited to a single nucleotide. This propensity of the coupled enzymatic reactions of Pol δ and Fen1, and in particular that of Pol δ3, are relevant in terms of the limitations of the cleavage specificity of Fen1 for short flaps, and acts to suppress the generation of longer flaps that require the intervention of the long flap pathway.

It is noted that these data reveal the spectrum of cleavage products, but only indirectly provide information on the actual cleavage site usage of Fen1. The specificity of Fen1 on preformed flap substrates has been extensively investigated and indicates a preference for short flaps of 2–8 nts [10], with a "flap+1" specificity. With the preformed flaps the flap junction is fixed, and thus this reflects cleavage at 1 nt past the junction. Fen1 displays flap cleavage at the flap junction, as well as at the flap-1 position, depending on the experimental conditions [47,48]. We have confirmed that our recombinant Fen1 preparations exhibit the flap+1 specificity under the conditions used in our experiments. At face value, this specificity does not explain the preponderance of the 1 nt product, since a preformed 1 nt flap substrate yields a 2 nt product. However, in an extensive analysis using both 3' and 5' flaps, it has been shown that the preferred substrate for yeast Fen1 is a double flap having a 1 nt 3'flap [49]. The origin of the 1 nt product can be explained since a 1 nt 5' flap can equilibrate to a 1 nt 3' flap, leaving a nick. Substrates with this structure yield a 1 nt Fen1 cleavage product [49]. (See Appendix A, Fig. A1 for a diagrammatic explanation).

The experiments of Fig. 4 provide an analysis only of the first flap cleavage during the combined Pol δ+Fen1 reactions. In order to obtain information on the subsequent flap cleavages, experiments were performed with the substrates where the 5'-blocking oligonucleotide was labeled at the 3' end. Two substrates were used, where the 5'-blocking oligonucleotide was preceded by a preformed 10nt flap ($F_{10}D_{17}$, Fig. 7A) or a 2 nt flap (F_2D_{17}, Fig. 7B). The analysis was performed with 20 nM Pol δ3 and 100 nM Fen1. The phosphorimage of the labeled products for the $F_{10}D_{17}$ (Fig. 7C) shows that Fen1 exhibits the expected preference for flap+1 cleavage alone or in combination with PCNA to produce a 16mer. Similarly, a 16mer is generated by cleavage of the F_2D_{17} substrate (Fig. 7D). For both substrates, the subsequent cleavages yield the 15mer and smaller products to form a ladder with a periodicity of 1 nt, which is consistent with consecutive single nucleotide cleavages as shown by the gradual decrease in intensity of the bands. These data illustrate the predominance of the single nucleotide product formation by Pol δ3/Fen1, consistent with a nick translation process.

3.6. The Ligation Step of Okazaki Fragment Processing

The final step of Okazaki fragment processing is nick ligation by DNA ligase I [5]. In order to complete the reconstitution of Okazaki fragment processing, we examined the efficiency of the ligation of the nicks generated during the Pol δ4/Fen1 and Pol δ3/Fen1 reactions by human DNA ligase I. For these experiments we used the Gap-D_{20} substrate (Fig. 8A) in which the blocking oligonucleotide was labeled at the 5'-end (Fig. 8A). We first compared Pol δ4 and Pol δ3 in promoting ligation at the initial ligation step in the absence of Fen1 (Fig. 8A). Only the ligation at the first encounter with the end of the 5'-blocking 20mer results in a labeled product. Ligation occurs much more readily with Pol δ3 than Pol δ4 (Fig. 8B). Quantitative analysis of the 70mer ligation products shows that at the 5 min time point, *ca.* the amount of ligated product was 8% when Pol δ3 was used as opposed to *ca.* 1% with Pol δ4 (not shown). These results are consistent with the different behavior of the two polymerases in strand displacement, where Pol δ4 readily performs strand displacement, while Pol δ3 stalls at the nick and idles (Fig. 2). The importance of the propensity of yeast Pol δ for maintaining a nick has been well established, and is not exhibited by yeast Pol ε [16].

Next, we examined the effects of varying the concentrations of Fen1 with a fixed amount of DNA ligase I using the same substrate. The phosphorimage of the labeled 70mer ligation products (Fig. 8C, showing only the 10 nM and 50 nM Fen1 reactions) reveals that formation of the ligation product was inhibited with increasing Fen1 concentrations with both polymerases, but was more evident with Pol δ3. The 70mer bands were quantitated, and plotted against time. In the case of Pol δ4, only <1% of ligated product was formed under all

Fen1 concentrations, and was lowest with 50 nM Fen1 (Fig. 8D). In the case of Pol δ3, the reaction was most rapid at 5 nM Fen1 (ca. 8% at 5 min), and was clearly inhibited as the Fen1 concentration increased (Fig. 8E). This decrease is likely due to competition of Fen1 with DNA ligase I for occupancy of PCNA. This in turn supports a model in which a complex of Pol δ3/Fen1/PCNA performs the strand removal, to be replaced by a Pol δ3/DNA ligase I/PCNA complex.

The 5'-end labeled Gap-D_{20} substrate used above measures a single defined reaction, that of ligation on the initial encounter with the 5'-blocking oligonucleotide. The very low efficiencies of ligation thus do not necessarily reflect on the overall efficiencies of Pol δ4 and Pol δ3 as this could occur in subsequent rounds of the Pol δ/Fen1 excision of the 5'-blocking oligonucleotide. In order to compare the efficiencies of Pol δ4 and Pol δ3 in promoting ligation, we utilized the Gap-D_{21} substrate, which was labeled at the 3' end instead of the 5' end (Fig. 8F). With this substrate, all the products formed by ligation during the Pol δ/Fen1 processing of the 21mer are captured as the 70mer; intermediates of the primer extension are not labeled, and the unligated cleavage products would be <21 nts. Analysis of the 70mer products (Fig. 8G) shows that processing/ligation reactions with both Pol δ4 and Pol δ3 were robust. Quantitation of the data showed that the reactions reached a maximum by about 100s, at *ca.* 28% for the reactions with Pol δ4 and *ca.* 18% for Pol δ3, respectively (Fig. 8H). Thus, it can be concluded that both Pol δ4 and Pol δ3 are competent in Okazaki fragment processing in a reconstituted system, even though their different properties result in qualitative differences in the ultimate distribution of cleavage products (Fig. 4).

3.7. The coupling of Pol δ and Fen1 reactions

An important question is whether the reactions of Pol δ, Fen1 and DNA ligase are simply stochastic, where they compete for binding to PCNA, or whether there is an inherent or physical basis for their coupling. This has been demonstrated in the archaeal model, where Pol1B, Fen1 and DNA ligase (Lig1) form a multi-protein complex with PCNA. Archaeal PCNA is a heterotrimer and each of the PCNA subunits has a specificity for binding of either PolB1, Fen1 or Lig1. Since each of the enzymes must not only bind to PCNA but to the DNA substrate, they must have conformational flexibility where they can swing away from the face of PCNA [25–28]. Human Fen1 exhibits multiple conformations on PCNA [50]. Structures of human DNA ligase I show that it also has an extended conformation, but it has been noted that in the closed conformation it also occludes the face of PCNA [4,5]. There is some biochemical evidence that yeast Pol δ may adopt different conformations on binding to PCNA [51]. An important limitation is that unlike archaeal PCNA, eukaryotic PCNA is a homotrimer. Human Pol δ exhibits multivalent interactions with PCNA, and at least three of its subunits (p125, p68 and p12) interact with PCNA (reviewed in [32]). Moreover, the p12 subunit possesses a PIP-box that is an extended one that functions as a PIP-degron by a high affinity binding to PCNA [39]. Currently, there is no biochemical evidence for the formation of higher complexes involving Pol δ, Fen1 or DNA ligase on PCNA. Thus, the full applicability of the archaeal model to higher eukaryotes seems doubtful. However, this does not preclude the possibility that this model has partial applicability to the eukaryotic system. It is also noted that multiple rounds of Pol δ and Fen1 reactions are involved, where the advantages of a coupling or "hand-off" process can be seen, while the ligation reaction is a terminal event.

We propose a working hypothesis that Pol δ 3 or Pol δ 4 are both resident on PCNA with Fen1 during the process of primer extension and replacement of the 5'-end of the Okazaki fragment. Our findings provide some insights into the applicability of such a model, since the combined reactions of Pol δ and Fen1 would be expected to exhibit alterations that reflect their physical coupling and affect the expected outcomes of their behavior based on

analysis of their individual reactions. The working model we propose is shown in Fig. 9, where Pol δ and Fen1 are shown bound to PCNA, with Pol δ utilizing two of the three PIP-box binding pockets [52] of PCNA, with Fen1 using the third. The DNA substrate is also shown, and the reaction cycle starts with Pol δ bound to PCNA and to the nick substrate, with Fen1 attached in a conformation that does not sterically hinder the access of Pol δ to the DNA. The reaction cycle starts with strand displacement by Pol δ to create a flap (Fig. 9, "1"). Next, Pol δ dissociates from the DNA substrate, and is replaced by Fen1 (Fig. 9, "2" and "3"). Fen1 then cleaves the flap (Fig.9, "4"), leaving a nicked DNA substrate. Fen1 then dissociates and is replaced by Pol δ (Fig.9, "4"). Viewed in this manner, it is seen that there is a cyclic switching of Pol δ and Fen1. Furthermore, each enzyme produces a product that is a substrate for the other. It should be noted that the binding affinity of the two enzymes for the DNA would be expected to make a significant contribution to their binding to the PCNA-DNA substrate, which dynamically switches between the PCNA-DNA-nick and the PCNA-DNA-flap structures. These changes in structure of the DNA could provide a thermodynamic basis for enabling the rapid switching of Pol δ and Fen1. This could be important in limiting the strand displacement reaction of Pol δ4.

One of the key features of the Pol δ 3-Fen1 combined reaction is that the rates of the reactions is not affected by Fen1 concentration (Figs. 4, 6). This is consistent with what would be expected of a coupled reaction that is shown in the model. The behavior of Pol δ 3 is in contrast to that of Pol δ 4 (*cf.* Figs. 4, 5). For Pol δ4, at low Fen1 concentrations, the flap cleavage products represent a range from 1–8 nts, reflecting the flap cleavage specificity of Fen1. However, as Fen1 concentration is increased, the pattern of products changes to one where shorter products, mainly mononucleotides are formed, and resembles that of Pol δ 3. This behavior is consistent with a stochastic process, where both Pol δ 4 and Fen1 are not resident together on PCNA and the size distribution is dependent on the rates of strand displacement before Pol δ4 is displaced by Fen1 (Section 3.5). However, this does not preclude the possibility that Pol δ4 is also acting in the context of a ternary complex in the model given in Fig. 9, for reasons discussed below.

Considerations of whether Pol δ 4 and Pol δ 3 can share occupancy of PCNA with Fen1 must take into account the multivalent interactions of Pol δ with PCNA. The p12 subunit of Pol δ functionally interacts with PCNA [32], and possesses a C-terminally extended PIP-box with high affinity for PCNA [39]. Its loss by removal of the p12 subunit in Pol δ 3 may facilitate the loading of Fen1 to form a ternary complex with PCNA by comparison to Pol δ 4. Thus, the transition of product formation by Pol δ 4/Fen1 can be argued to reflect the higher concentrations of Fen1 that are required for the formation of the Pol δ 4/Fen1/PCNA complex, in a situation where it may be competing with p12 for interaction with PCNA. We have previously noted the importance of the differences in Pol δ 4 and Pol δ 3 that are occasioned by the loss of the p12-PCNA interaction in regard to switching reactions with translesion polymerases [32,53].

The basis for the termination of the Pol δ /Fen1 reactions and the switch to the ligation reaction is still a mystery, *i.e.*, how does the system sense when sufficient replacement of the 5'end of the Okazaki fragment is sufficient for the removal of the *ca*. 30 nts representing the RNA/DNA pimer. The foregoing discussions lead to a novel consideration. If Pol δ 4 or Pol δ 3 were to share occupancy of PCNA with Fen1, the processivity of the complex might be reduced compared to that of Pol δ in the unshared state. Thus, one possibility is that the inherent processivity of the complex may be what determines at which point the combined reactions of Pol δ /Fen1 terminates, leading to their dissociation and the recruitment of DNA ligase I.

Our data for the complete reactions containing Pol δ, Fen1 and DNA ligase I show that Fen1 competes with DNA ligase I (Fig. 8). This is consistent with a model in which a complex of Pol δ3/Fen1/PCNA performs the RNA/DNA primer removal, to be replaced by a Pol δ3/DNA ligase I/PCNA complex.

Finally, we note that our findings do not necessarily directly reflect the *in vivo* situation. However, it is a hallmark of DNA replication and repair processes that they involve formation of chromatin bound complexes, rather than stochastic processes. Our studies also point to avenues for further investigation that could provide evidence for formation of Pol δ / Fen/PCNA complexes.

3.8. Significance of our findings: A case for Pol δ3 as a participant in Okazaki fragment processing in the human system

Our previous studies had shown that Pol δ3 is formed in the cell in response to DNA damage, and analysis of its properties supported a role in DNA repair [32]. In an analysis of the distribution of all four subunits of Pol δ by laser scanning cytometry, we have obtained evidence that p12 levels are significantly reduced during the S phase, unlike the p125, p50 and p68 subunits [32,40], suggesting that Pol δ3 might also be formed during the replication phase of the cell cycle. More recently, we have shown that p12 levels are significantly reduced during the S phase by analysis of synchronized cell populations [39]. p12 degradation during the S phase was shown to be regulated by the $CRL4^{Cdt2}$ E3 ligase that plays an important role in cellular DNA replication during cell cycle progression by degradation of the licensing factor, Cdt1 as well as p21 and Set8 [54]. Additionally, the PIP-box responsible for the interaction of p12 with PCNA was shown to be an extended one that conforms to the PIP-degrons that are recognized by $CRL4^{Cdt2}$ [55]. That the formation of Pol δ3 is mediated by a central regulator of cell cycle progression adds weight to the concept of a potential role for Pol δ3 in DNA replication.

Our findings show that Pol δ3 has the near-ideal characteristics of a polymerase designed for Okazaki fragment processing with the important characteristics described by Burgers' laboratory in the context of yeast Pol δ [16,17] *viz.*, restricted strand displacement, idling and maintenance of a ligatable nick. Our studies reveal a strong bias toward the restriction of the coupled Pol δ/Fen1 cleavage reactions to removal of 1 or 2 nt fragments, in a near stringent manner with Pol δ3. This mode of operation suppresses the production of longer flaps, and acts preemptively to minimize the use of the long flap pathway which serves as a fail-safe against failures of Okazaki fragment maturation that can lead to genomic instability. Human Pol δ3, like yeast Pol δ, is a trimer with the same conserved subunits. Viewed in this manner, Pol δ3 may be regarded as a more highly evolved version of yeast Pol δ. Given that yeast Pol δ and human Pol δ3 are both composed of three subunits that are evolutionarily conserved, Pol δ3 (and not Pol δ4) may be considered as the ortholog of yeast Pol δ. However, it is noted that both yeast Pol δ and human Pol δ4 exhibit significant abilities for strand displacement, unlike Pol δ3. It is also noted that the same qualities of Pol δ3 that appear to be appropriate for its role in DNA repair – increased stalling/idling and increased proofreading/fidelity - are also appropriate for a role in Okazaki fragment processing.

These findings now denote a potential role for Pol δ3 in higher eukaryotic DNA replication as a participant in Okazaki fragment processing. However, we cannot discount the possibility that Pol δ4 may also function in this role, as their abilities to generate ligated products in the complete reaction are comparable. This raises the question as to how and why Pol δ4 and Pol δ3 are deployed during DNA replication. Given the size and complexity of the human genome, and the complexity of human chromatin, it is possible that such considerations may dictate their differential utilization. In addition, it is possible that there

are as yet unknown protein factors that could modulate their functions or direct their utilization. One possibility why both may be involved could relate to a differential usage dictated by the nature of the template sequences they encounter [56,57]. Further studies are needed to establish the roles of Pol δ3 (and Pol δ4) in Okazaki fragment processing, but nevertheless it is clear that our studies have revealed a significant potential for the extension of the number of polymerases that may be required for the replication of the more complex higher eukaryotic genome. In addition, we cannot take for granted that Pol δ activity is solely involved in lagging strand and not in leading strand synthesis, as evidence for this is still incomplete in the human system [58], and there is evidence that the activities of Pol δ and Pol ε may operate in a partly independent manner during cellular DNA replication [59–62]

Supplementary Material

Refer to Web version on PubMed Central for supplementary material.

Acknowledgments

This work was supported by grants from the National Institutes of Health (GM31973 and ES14737) to M. Y. W. T. L.

Abbreviations

Pol	DNA polymerase
Fen1	flap endonuclease 1
PCNA	proliferating cell nuclear antigen
RFC	replication factor C
AP site	apurinic/apyrimidinic site

REFERENCES

1. Burgers PM. Polymerase dynamics at the eukaryotic DNA replication fork. J. Biol. Chem. 2009; 284:4041–4045. [PubMed: 18835809]
2. Balakrishnan L, Bambara RA. Okazaki fragment metabolism. Cold Spring Harb Perspect Biol. 2013; 5:a10173.
3. Zheng L, Shen B. Okazaki fragment maturation: nucleases take centre stage. J Mol Cell Biol. 2011; 3:23–30. [PubMed: 21278448]
4. Howes TR, Tomkinson AE. DNA ligase I, the replicative DNA ligase. Subcell Biochem. 2012; 62:327–341. [PubMed: 22918593]
5. Tomkinson AE, Vijayakumar S, Pascal JM, Ellenberger T. DNA ligases: structure, reaction mechanism, and function. Chem Rev. 2006; 106:687–699. [PubMed: 16464020]
6. Mocquet V, Laine JP, Riedl T, Yajin Z, Lee MY, Egly JM. Sequential recruitment of the repair factors during NER: the role of XPG in initiating the resynthesis step. EMBO J. 2008; 27:155–167. [PubMed: 18079701]
7. Liu Y, Wilson SH. DNA base excision repair: a mechanism of trinucleotide repeat expansion. Trends Biochem. Sci. 2012; 37:162–172. [PubMed: 22285516]
8. Liu Y, Beard WA, Shock DD, Prasad R, Hou EW, Wilson SH. DNA polymerase beta and flap endonuclease 1 enzymatic specificities sustain DNA synthesis for long patch base excision repair. J. Biol. Chem. 2005; 280:3665–3674. [PubMed: 15561706]
9. Tsutakawa SE, Classen S, Chapados BR, Arvai AS, Finger LD, Guenther G, Tomlinson CG, Thompson P, Sarker AH, Shen B, Cooper PK, Grasby JA, Tainer JA. Human flap endonuclease

structures, DNA double-base flipping, and a unified understanding of the FEN1 superfamily. Cell. 2011; 145:198–211. [PubMed: 21496641]

10. Balakrishnan L, Bambara RA. FLAP Endonuclease 1. Annu. Rev. Biochem. 2013; 82:9.1–9.25.
11. Kang YH, Lee CH, Seo YS. Dna2 on the road to Okazaki fragment processing and genome stability in eukaryotes. Crit. Rev. Biochem. Mol. Biol. 2010; 45:71–96. [PubMed: 20131965]
12. Pike JE, Burgers PM, Campbell JL, Bambara RA. Pif1 helicase lengthens some Okazaki fragment flaps necessitating Dna2 nuclease/helicase action in the two-nuclease processing pathway. J. Biol. Chem. 2009; 284:25170–25180. [PubMed: 19605347]
13. Pike JE, Henry RA, Burgers PM, Campbell JL, Bambara RA. An alternative pathway for Okazaki fragment processing: resolution of fold-back flaps by Pif1 helicase. J. Biol. Chem. 2010; 285:41712–41723. [PubMed: 20959454]
14. Ayyagari R, Gomes XV, Gordenin DA, Burgers PM. Okazaki fragment maturation in yeast. I. Distribution of functions between FEN1 AND DNA2. J. Biol. Chem. 2003; 278:1618–1625. [PubMed: 12424238]
15. Jin YH, Ayyagari R, Resnick MA, Gordenin DA, Burgers PM. Okazaki fragment maturation in yeast. II. Cooperation between the polymerase and 3'–5'-exonuclease activities of Pol delta in the creation of a ligatable nick. J. Biol. Chem. 2003; 278:1626–1633. [PubMed: 12424237]
16. Garg P, Stith CM, Sabouri N, Johansson E, Burgers PM. Idling by DNA polymerase delta maintains a ligatable nick during lagging-strand DNA replication. Genes Dev. 2004; 18:2764–2773. [PubMed: 15520275]
17. Garg P, Burgers PM. How the cell deals with DNA nicks. Cell Cycle. 2005; 4:221–224. [PubMed: 15655350]
18. Stith CM, Sterling J, Resnick MA, Gordenin DA, Burgers PM. Flexibility of eukaryotic Okazaki fragment maturation through regulated strand displacement synthesis. J. Biol. Chem. 2008; 283:34129–34140. [PubMed: 18927077]
19. Nick McElhinny SA, Gordenin DA, Stith CM, Burgers PM, Kunkel TA. Division of labor at the eukaryotic replication fork. Mol. Cell. 2008; 30:137–144. [PubMed: 18439893]
20. Kunkel TA. Balancing eukaryotic replication asymmetry with replication fidelity. Curr Opin Chem Biol. 2011; 15:620–626. [PubMed: 21862387]
21. Bermudez VP, Farina A, Raghavan V, Tappin I, Hurwitz J. Studies on Human DNA Polymerase epsilon and GINS Complex and Their Role in DNA Replication. J. Biol. Chem. 2011; 286:28963–28977. [PubMed: 21705323]
22. Bermudez VP, Farina A, Tappin I, Hurwitz J. Influence of the human cohesion establishment factor Ctf4/AND-1 on DNA replication. J. Biol. Chem. 2010; 285:9493–9505. [PubMed: 20089864]
23. Im JS, Ki SH, Farina A, Jung DS, Hurwitz J, Lee JK. Assembly of the Cdc45-Mcm2-7-GINS complex in human cells requires the Ctf4/And-1, RecQL4, and Mcm10 proteins. Proc. Natl. Acad. Sci. U S A. 2009; 106:15628–15632. [PubMed: 19805216]
24. Moldovan GL, Pfander B, Jentsch S. PCNA, the maestro of the replication fork. Cell. 2007; 129:665–679. [PubMed: 17512402]
25. Beattie TR, Bell SD. Coordination of multiple enzyme activities by a single PCNA in archaeal Okazaki fragment maturation. EMBO J. 2012; 31:1556–1567. [PubMed: 22307085]
26. Pascal JM, Tsodikov OV, Hura GL, Song W, Cotner EA, Classen S, Tomkinson AE, Tainer JA, Ellenberger T. A flexible interface between DNA ligase and PCNA supports conformational switching and efficient ligation of DNA. Mol. Cell. 2006; 24:279–291. [PubMed: 17052461]
27. Dore AS, Kilkenny ML, Jones SA, Oliver AW, Roe SM, Bell SD, Pearl LH. Structure of an archaeal PCNA1-PCNA2-FEN1 complex: elucidating PCNA subunit and client enzyme specificity. Nucleic Acids Res. 2006; 34:4515–4526. [PubMed: 16945955]
28. Dionne I, Nookala RK, Jackson SP, Doherty AJ, Bell SD. A heterotrimeric PCNA in the hyperthermophilic archaeon Sulfolobus solfataricus. Mol. Cell. 2003; 11:275–282. [PubMed: 12535540]
29. Lee MY, Jiang YQ, Zhang SJ, Toomey NL. Characterization of human DNA polymerase delta and its immunochemical relationships with DNA polymerase alpha and epsilon. J. Biol. Chem. 1991; 266:2423–2429. [PubMed: 1703528]

30. Mo J, Liu L, Leon A, Mazloum N, Lee MY. Evidence that DNA polymerase delta isolated by immunoaffinity chromatography exhibits high-molecular weight characteristics and is associated with the KIAA0039 protein and RPA. Biochemistry. 2000; 39:7245–7254. [PubMed: 10852724]

31. Liu L, Mo J, Rodriguez-Belmonte EM, Lee MY. Identification of a fourth subunit of mammalian DNA polymerase delta. J. Biol. Chem. 2000; 275:18739–18744. [PubMed: 10751307]

32. Lee MY, Zhang Z, Lin SH, Chea J, Wang X, LeRoy C, Wong A, Zhang Z, Lee EY. Regulation of human DNA polymerase Delta in the cellular responses to DNA damage. Environ Mol Mutagen. 2012; 53:683–698. [PubMed: 23047826]

33. Xie B, Mazloum N, Liu L, Rahmeh A, Li H, Lee MY. Reconstitution and characterization of the human DNA polymerase delta four-subunit holoenzyme. Biochemistry. 2002; 41:13133–13142. [PubMed: 12403614]

34. Zhou Y, Meng X, Zhang S, Lee EY, Lee MY. Characterization of human DNA polymerase delta and its subassemblies reconstituted by expression in the multibac system. PLoS ONE. 2012; 7:e39156. [PubMed: 22723953]

35. Zhang S, Zhou Y, Trusa S, Meng X, Lee EY, Lee MY. A novel DNA damage response: rapid degradation of the p12 subunit of dna polymerase delta. J. Biol. Chem. 2007; 282:15330–15340. [PubMed: 17317665]

36. Meng X, Zhou Y, Zhang S, Lee EY, Frick DN, Lee MY. DNA damage alters DNA polymerase delta to a form that exhibits increased discrimination against modified template bases and mismatched primers. Nucleic Acids Res. 2009; 37:647–657. [PubMed: 19074196]

37. Meng X, Zhou Y, Lee EY, Lee MY, Frick DN. The p12 subunit of human polymerase delta modulates the rate and fidelity of DNA synthesis. Biochemistry. 2010; 49:3545–3554. [PubMed: 20334433]

38. Garg P, Burgers PM. DNA polymerases that propagate the eukaryotic DNA replication fork. Crit. Rev. Biochem. Mol. Biol. 2005; 40:115–128. [PubMed: 15814431]

39. Zhang S, Zhao H, Darzynkiewicz Z, Zhou P, Zhang Z, Lee EY, Lee MY. A Novel Function of CRL4Cdt2: Regulation of the Subunit Structure of DNA Polymerase δ in Response to DNA Damage and During the S phase. J. Biol. Chem. 2013 under revision.

40. Chea J, Zhang S, Zhao H, Zhang Z, Lee EY, Darzynkiewicz Z, Lee MY. Spatiotemporal recruitment of human DNA polymerase delta to sites of UV damage. Cell Cycle. 2012; 11:2885–2895. [PubMed: 22801543]

41. Zhang S, Chea J, Meng X, Zhou Y, Lee EY, Lee MY. PCNA is ubiquitinated by RNF8. Cell Cycle. 2008; 7:3399–3404. [PubMed: 18948756]

42. Li H, Xie B, Zhou Y, Rahmeh A, Trusa S, Zhang S, Gao Y, Lee EY, Lee MY. Functional roles of p12, the fourth subunit of human DNA polymerase delta. J. Biol. Chem. 2006; 281:14748–14755. [PubMed: 16510448]

43. Johnson KA. Conformational coupling in DNA polymerase fidelity. Annu. Rev. Biochem. 1993; 62:685–713. [PubMed: 7688945]

44. Khare V, Eckert KA. The proofreading 3'–5' exonuclease activity of DNA polymerases: a kinetic barrier to translesion DNA synthesis. Mutat. Res. 2002; 510:45–54. [PubMed: 12459442]

45. Kunkel TA, Bebenek K. DNA replication fidelity. Annu. Rev. Biochem. 2000; 69:497–529. [PubMed: 10966467]

46. Sebesta M, Burkovics P, Juhasz S, Zhang S, Szabo JE, Lee MY, Haracska L, Krejci L. Role of PCNA and TLS polymerases in D-loop extension during homologous recombination in humans. DNA Repair (Amst). 2013

47. Harrington JJ, Lieber MR. DNA structural elements required for FEN-1 binding. J. Biol. Chem. 1995; 270:4503–4508. [PubMed: 7876218]

48. Harrington JJ, Lieber MR. The characterization of a mammalian DNA structure-specific endonuclease. EMBO J. 1994; 13:1235–1246. [PubMed: 8131753]

49. Kao HI, Henricksen LA, Liu Y, Bambara RA. Cleavage specificity of Saccharomyces cerevisiae flap endonuclease 1 suggests a double-flap structure as the cellular substrate. J. Biol. Chem. 2002; 277:14379–14389. [PubMed: 11825897]

50. Sakurai S, Kitano K, Yamaguchi H, Hamada K, Okada K, Fukuda K, Uchida M, Ohtsuka E, Morioka H, Hakoshima T. Structural basis for recruitment of human flap endonuclease 1 to PCNA. EMBO J. 2005; 24:683–693. [PubMed: 15616578]
51. Netz DJ, Stith CM, Stumpfig M, Kopf G, Vogel D, Genau HM, Stodola JL, Lill R, Burgers PM, Pierik AJ. Eukaryotic DNA polymerases require an iron-sulfur cluster for the formation of active complexes. Nat Chem Biol. 2012; 8:125–132. [PubMed: 22119860]
52. Gulbis JM, Kelman Z, Hurwitz J, O'Donnell M, Kuriyan J. Structure of the C-terminal region of p21(WAF1/CIP1) complexed with human PCNA. Cell. 1996; 87:297–306. [PubMed: 8861913]
53. Zhang Z, Zhang S, Lin SH, Wang X, Wu L, Lee EY, Lee MY. Structure of monoubiquitinated PCNA: Implications for DNA polymerase switching and Okazaki fragment maturation. Cell Cycle. 2012; 11:2128–2136. [PubMed: 22592530]
54. Abbas T, Dutta A. CRL4Cdt2: master coordinator of cell cycle progression and genome stability. Cell Cycle. 2011; 10:241–249. [PubMed: 21212733]
55. Havens CG, Walter JC. Mechanism of CRL4(Cdt2), a PCNA-dependent E3 ubiquitin ligase. Genes Dev. 2011; 25:1568–1582. [PubMed: 21828267]
56. Hile SE, Wang X, Lee MY, Eckert KA. Beyond translesion synthesis: polymerase kappa fidelity as a potential determinant of microsatellite stability. Nucleic Acids Res. 2012; 40:1636–1647. [PubMed: 22021378]
57. Shah SN, Opresko PL, Meng X, Lee MY, Eckert KA. DNA structure and the Werner protein modulate human DNA polymerase delta-dependent replication dynamics within the common fragile site FRA16D. Nucleic Acids Res. 2010; 38:1149–1162. [PubMed: 19969545]
58. Pavlov YI, Shcherbakova PV. DNA polymerases at the eukaryotic fork-20 years later. Mutat Res. 2010; 685:45–53. [PubMed: 19682465]
59. Fuss J, Linn S. Human DNA polymerase epsilon colocalizes with proliferating cell nuclear antigen and DNA replication late, but not early, in S phase. J. Biol. Chem. 2002; 277:8658–8666. [PubMed: 11741962]
60. Rytkonen AK, Vaara M, Nethanel T, Kaufmann G, Sormunen R, Laara E, Nasheuer HP, Rahmeh A, Lee MY, Syvaoja JE, Pospiech H. Distinctive activities of DNA polymerases during human DNA replication. FEBS J. 2006; 273:2984–3001. [PubMed: 16762037]
61. Vaara M, Itkonen H, Hillukkala T, Liu Z, Nasheuer HP, Schaarschmidt D, Pospiech H, Syvaoja JE. Segregation of Replicative DNA Polymerases during S Phase: DNA Polymerase epsilon but not DNA Polymerases alpha/delta, are associated with Lamins throughout S phase in human Cells. J. Biol. Chem. 2012; 287:33327–33338. [PubMed: 22887995]
62. Prindle MJ, Loeb LA. DNA polymerase delta in DNA replication and genome maintenance. Environ Mol Mutagen. 2012; 53:666–682. [PubMed: 23065663]

Highlights

- Two forms of human Pol δ were characterized in a reconstituted system
- Pol δ4 exhibits strong strand displacement activity in contrast to Pol δ3
- Primary cleavage products in the coupled Pol δ/Fen1 reactions were mononucleotides
- Pol δ3 exhibits near-ideal properties for a role in Okazaki fragment processing
- These studies support the novel concept that Pol δ3 participates in DNA replication

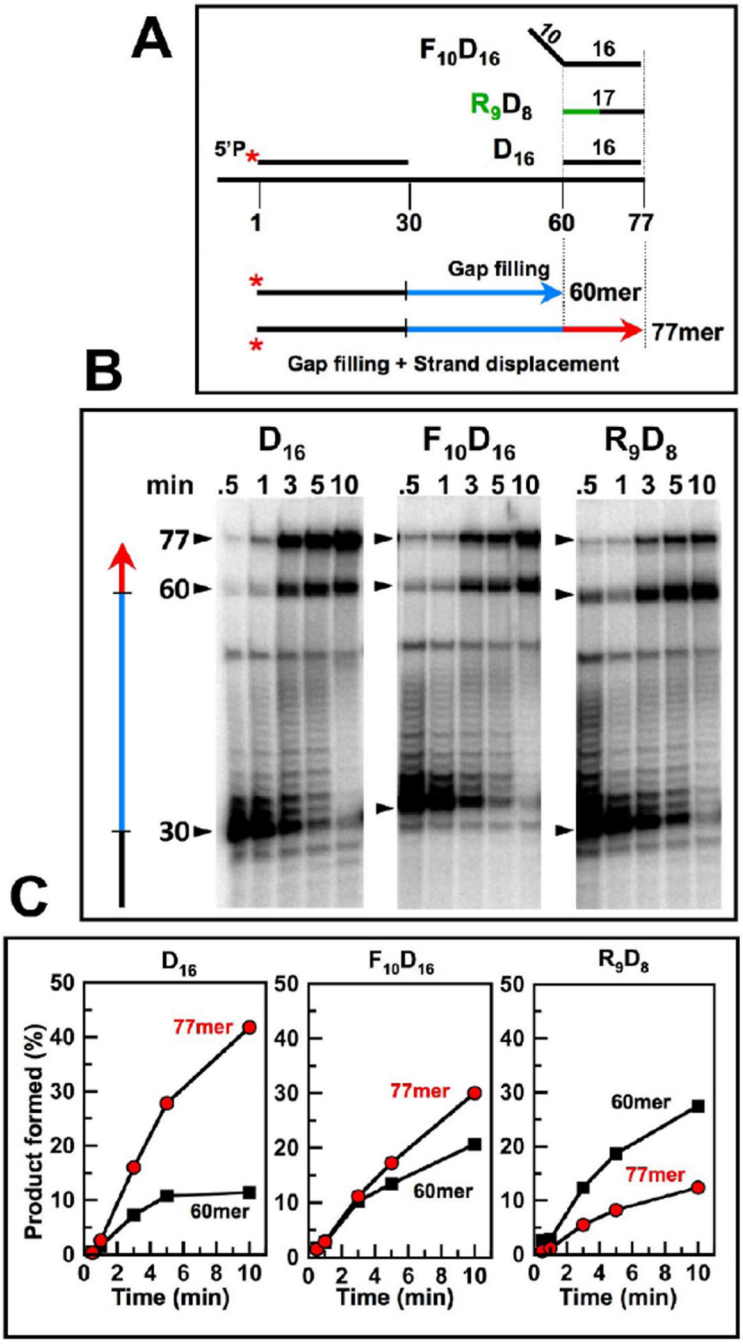

Figure 1. Strand displacement of DNA and RNA 5'-blocking oligonucleotides by Pol δ4

(A) Diagram of oligonucleotide substrates with different blocking sequences (see text). (B) 100 nM selected oligonucleotide DNA was incubated with 10 nM Pol δ and 400 nM PCNA in 50 mM Tris-HCl pH 6.5 and 25 mM NaCl. The reaction was quenched at 0.5, 1, 3, 5 and 10 min and analyzed by sequencing gel electrophoresis (Materials and Methods). The main products are 60mer and 77mer. The formation of 77mer dictates the occurrence of Pol δ strand displacement synthesis. (C) The amounts of 60mer (squares) and 77mer (circles) were quantified as a percentage of the original primer and plotted against time.

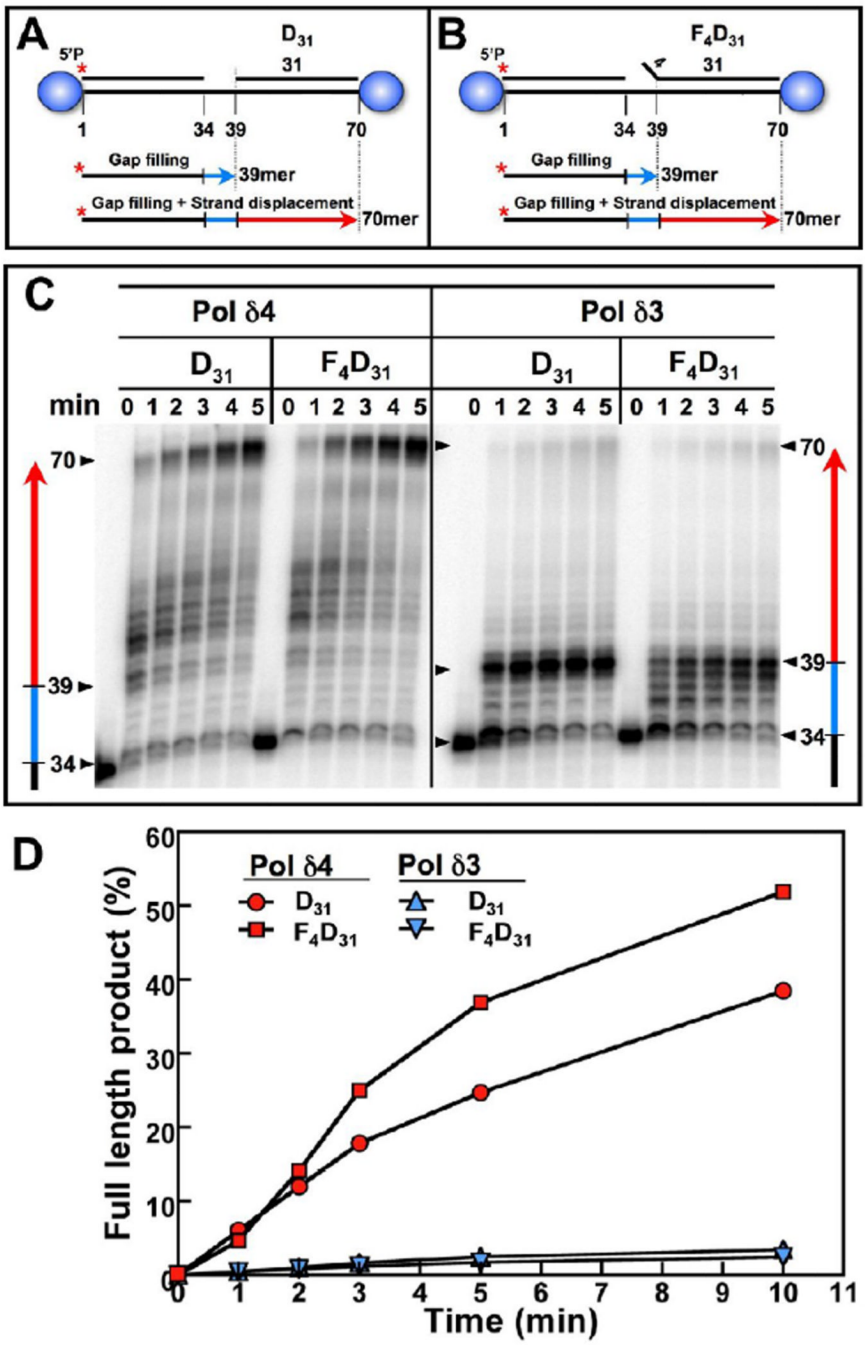

Figure 2. Strand displacement by Pol δ4 and Pol δ3 on DNA substrates with or without a flap

(A) Diagram of the D_{31} substrate. The templates were biotinylated at both ends and blocked with streptavidin, shown as the shaded circle. (B) diagram of the F_4D_{31} substrate. (C) Analysis of the strand displacement products produced by Pol δ4 (left panel) and Pol δ3 (right panel) by gel electrophoresis with the D_{31} and F_4D_{31} substrates. The final reaction mixture contained 20 nM Pol δ, 50 nM DNA, 10 nM RFC, 70 nM PCNA, 50 mM Bis-Tris (pH 6.5), 30 mM NaCl, 2mM DTT, 0.2 mg/ml BSA, 1 mM ATP, 5 mM $MgCl_2$, and 0.05 mM dNTP. The DNA substrates were incubated with streptavidin to block both ends before loading of the PCNA and DNA polymerase onto the DNA substrate. Reactions were started by adding $MgCl_2$ and dNTP, and quenched at 1, 2, 3, 4, 5 min. (D) The amounts of the full

length 70mer were quantitated and expressed as a percentage of the starting primer and plotted with time. Data for Pol δ4 are shown as circles (D_{31} substrate) and squares (F_4D_{31} substrate); data for Pol δ3 are shown as triangles (D_{31} substrate) and inverted triangles (F_4D_{31} substrate).

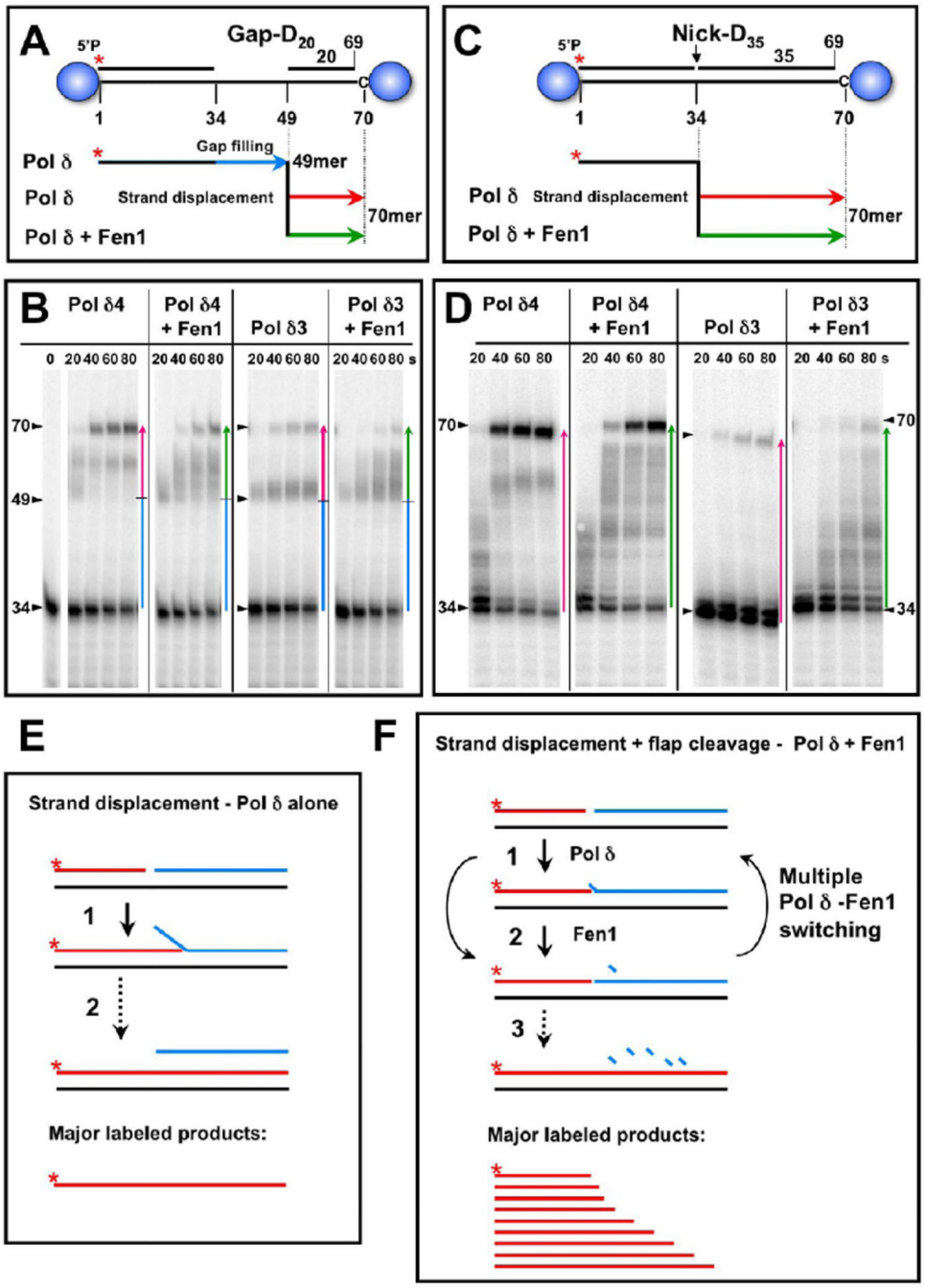

Figure 3. Analysis of the combined actions of Pol δ4/Fen1 and Pol δ3/Fen1 in strand displacement/flap cleavage as revealed by extension of a 5'-[^{32}P]end labeled primer

(A), (C) Diagrams of the Gap-D_{20} and Nick-D_{35} substrates. (B) Gap-D_{20} DNA (20 nM) was blocked with streptavidin and then loaded with 40 nM PCNA by 20 nM RFC. The primer extension reactions were initiated by the addition of 50 nM Pol δ4 or Pol δ3 in the absence or presence of 100 nM Fen1. The reactions were quenched at 20, 40, 60 and 80 sec and visualized by phosphorimaging after sequence gel electrophoresis. Product formation by Pol δ4 is shown in the absence (first panel) and presence 100 nM Fen1 (second panel). Product formation by Pol δ3 is shown in the absence (third panel) and presence 100 nM Fen1 (fourth panel). D) The Nick-D_{35} substrate was used and reaction condition were identical to those

used in B. Panels shown in B and D were run on the same gel. (E) Diagram of the strand displacement reaction by Pol δ alone. “1” Strand displacement results in the formation of a flap. In the case of Pol δ4, this reaction proceeds without much interruption to generate the full length 70mer as the major product. (F) Diagram of the combined reactions of Pol δ and Fen1. “1” Pol δ initiates strand displacement, and Fen1 then cleaves off the flap “2”. This leads to a stepwise extension of the labeled primer which appears as a ladder of intermediate products.

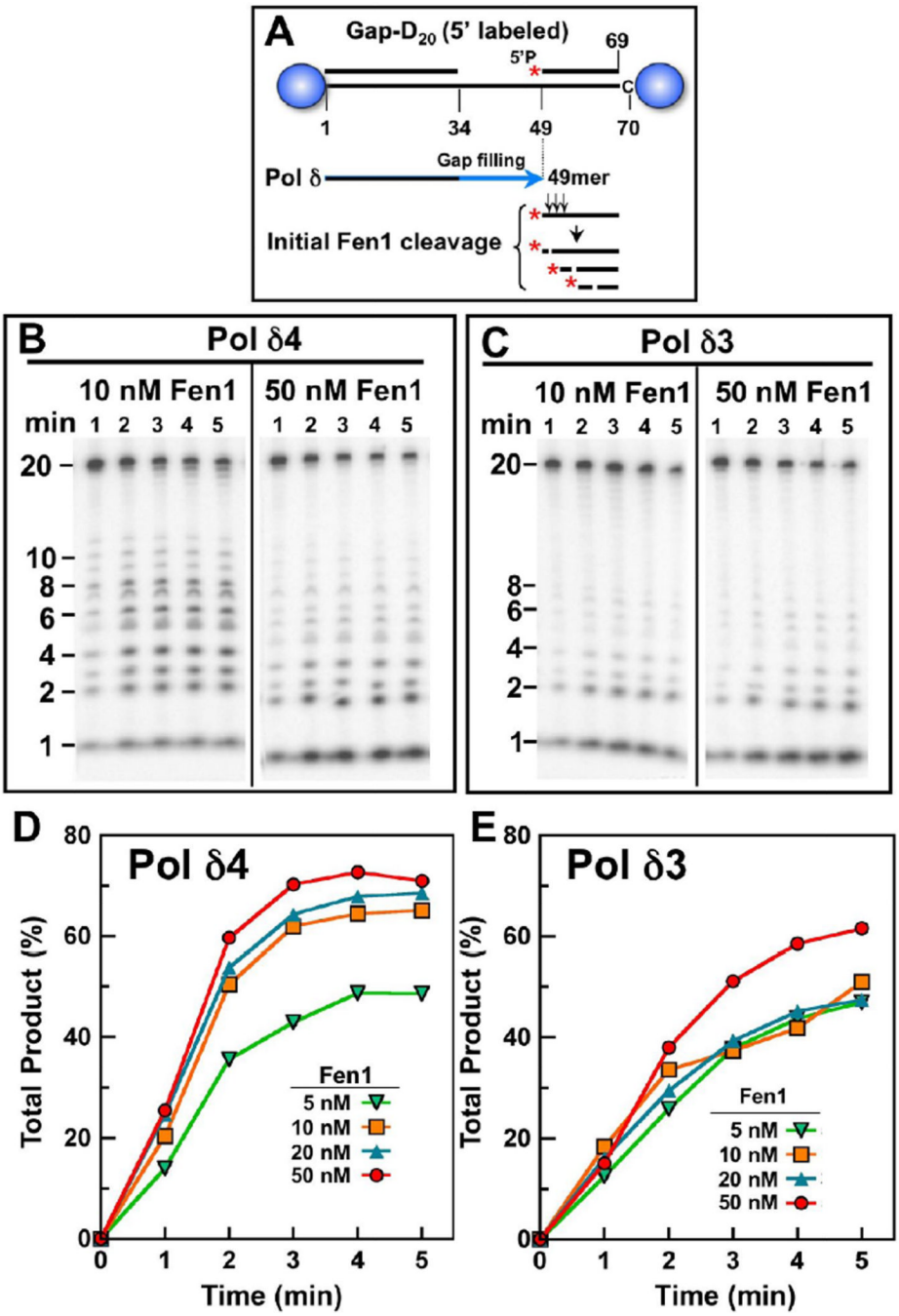

Figure 4. Analysis of the combined actions of Pol δ/Fen1 and Pol δ3/Fen1 in strand displacement/ flap cleavage as revealed by progressive degradation of a 5'-[^{32}P]end labeled blocking oligonucleotide

(A) Diagram of the Gap-D_{20} substrate. (B), (C) 20 nM biotinylated oligo DNA was blocked with 50 nM streptavidin and then loaded with PCNA (40 nM) by 20 nM RFC. The reactions were initiated by the addition of 20 nM Pol δ4 or Pol δ3 in the presence of 5, 10, 20 or 50 nM Fen1 at 37°C. The reactions were quenched at 1, 2, 3, 4, and 5 min. Representative gels for the reactions containing 10 nM or 50 nM Fen1 are shown for Pol δ4 (B), and Pol δ3 (C). (D), (E) The individual oligonucleotide products of the reactions were quantitated, and the total product formation (1–10 nts) for each time point were calculated and plotted against

time for Pol δ4 (D) and Pol δ3 (E). Product formation for the 5, 10, 20 and 50 nM Fen1 are indicated by inverted triangle, squares, triangles and circles, respectively.

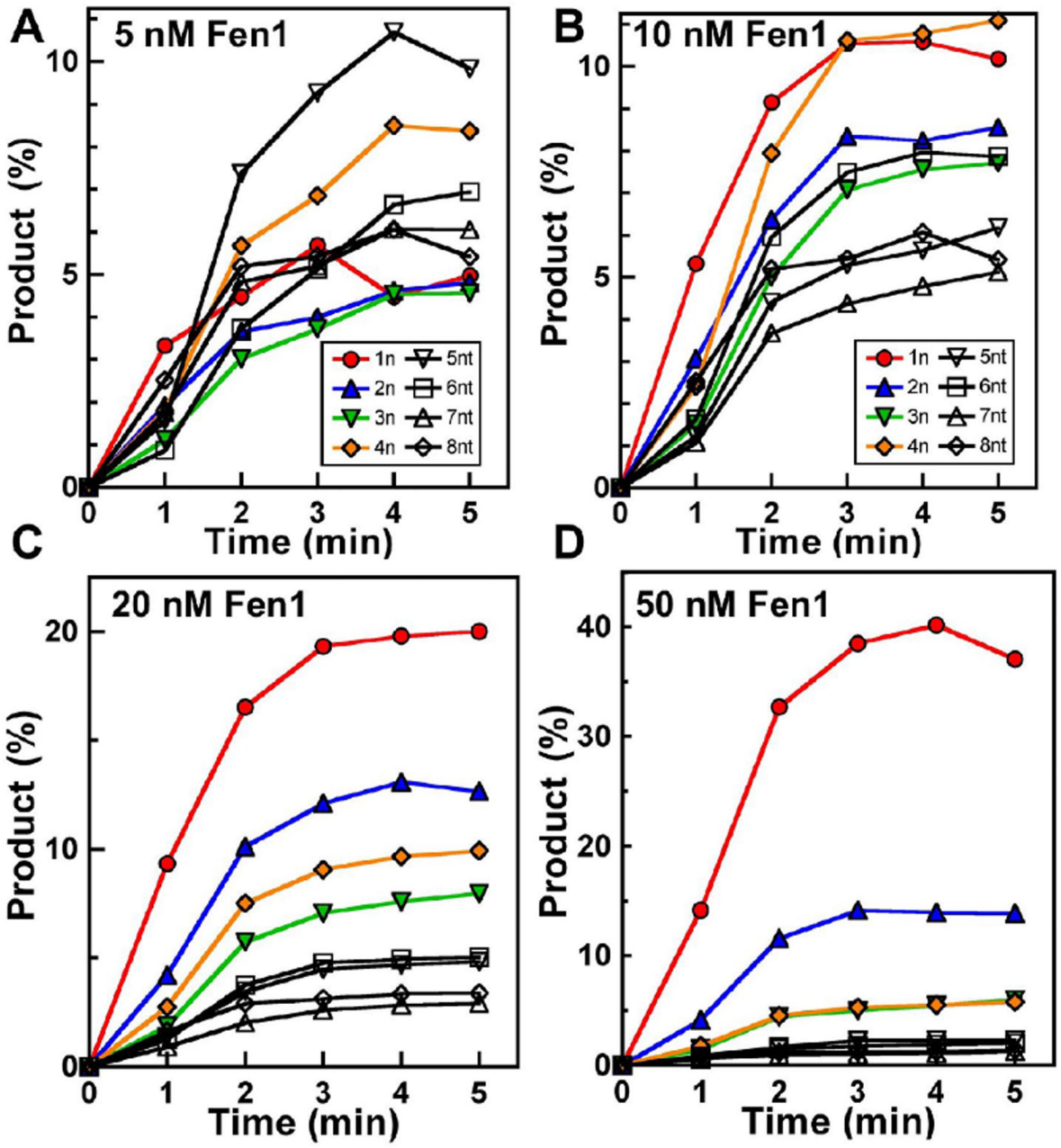

Fig. 5. Time course of formation of individual cleavage fragments by Pol δ4/Fen1

Data from the experiment shown in Fig. 4 at different Fen1 concentrations were plotted against time. (A) 5 nM Fen1. (B) 10 nM Fen1. (C) 20 nM Fen1. (D) 50 nM Fen1. Data for the cleavage fragments from 1 – 8 nts are shown as: 1 nt, filled circles; 2 nt, filled triangles; 3 nt, filled inverted triangles; 4 nt, filled diamonds; 5 nt, open inverted triangles; 6 nt, open squares; 7 nt, open triangles; 8 nt, open diamonds.

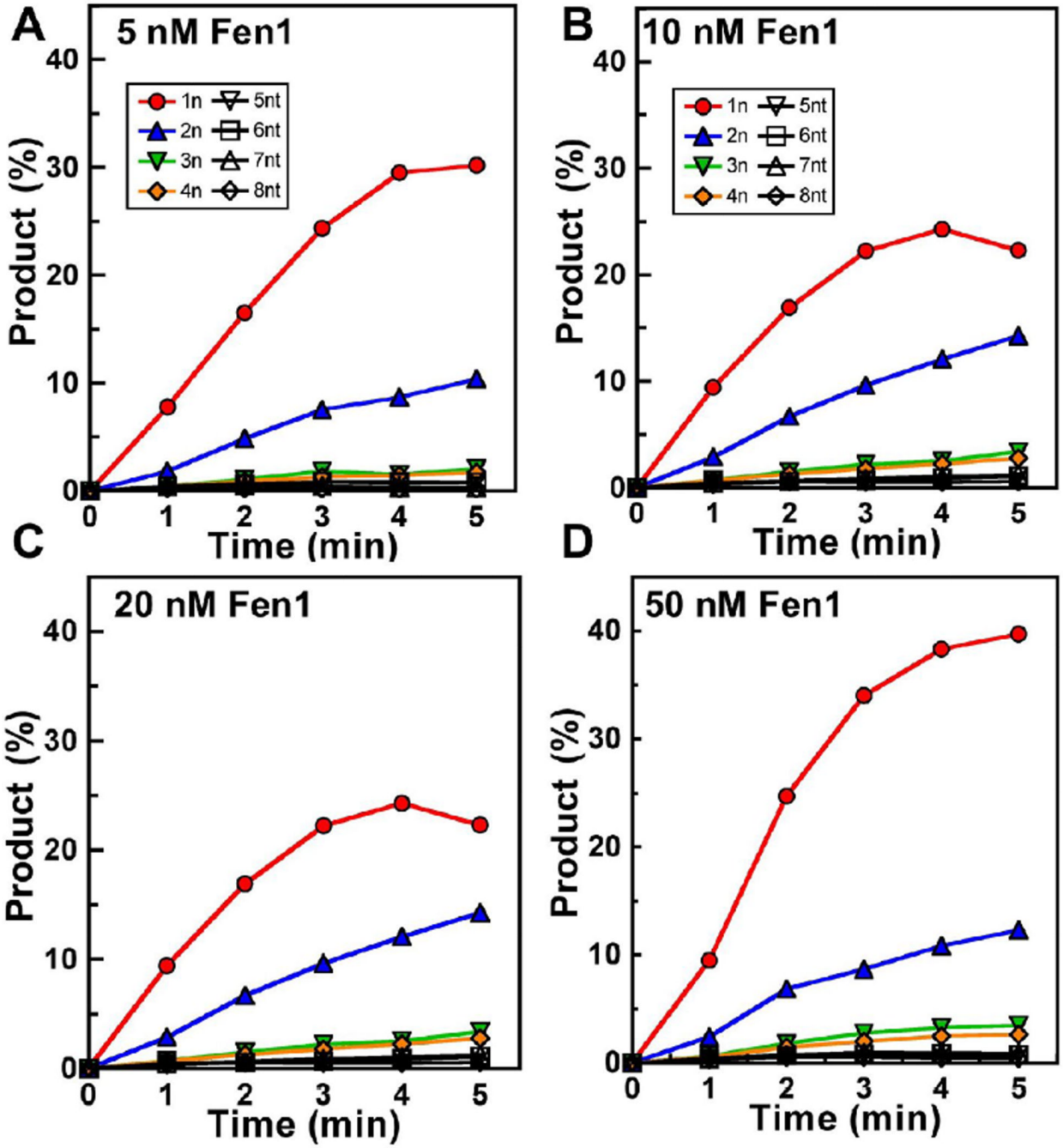

Fig. 6. Time course of formation of individual cleavage fragments by Pol δ3/Fen1

Data from the experiment shown in Fig. 4 at different Fen1 concentrations were plotted against time. (A) 5 nM Fen1. (B) 10 nM Fen1. (C) 20 nM Fen1. (D) 50 nM Fen1. Data for the cleavage fragments from 1 – 8 nts are shown as: 1 nt, filled circles; 2 nt, filled triangles; 3 nt, filled inverted triangles; 4 nt, filled diamonds; 5 nt, open inverted triangles; 6 nt, open squares; 7 nt, open triangles; 8 nt, open diamonds.

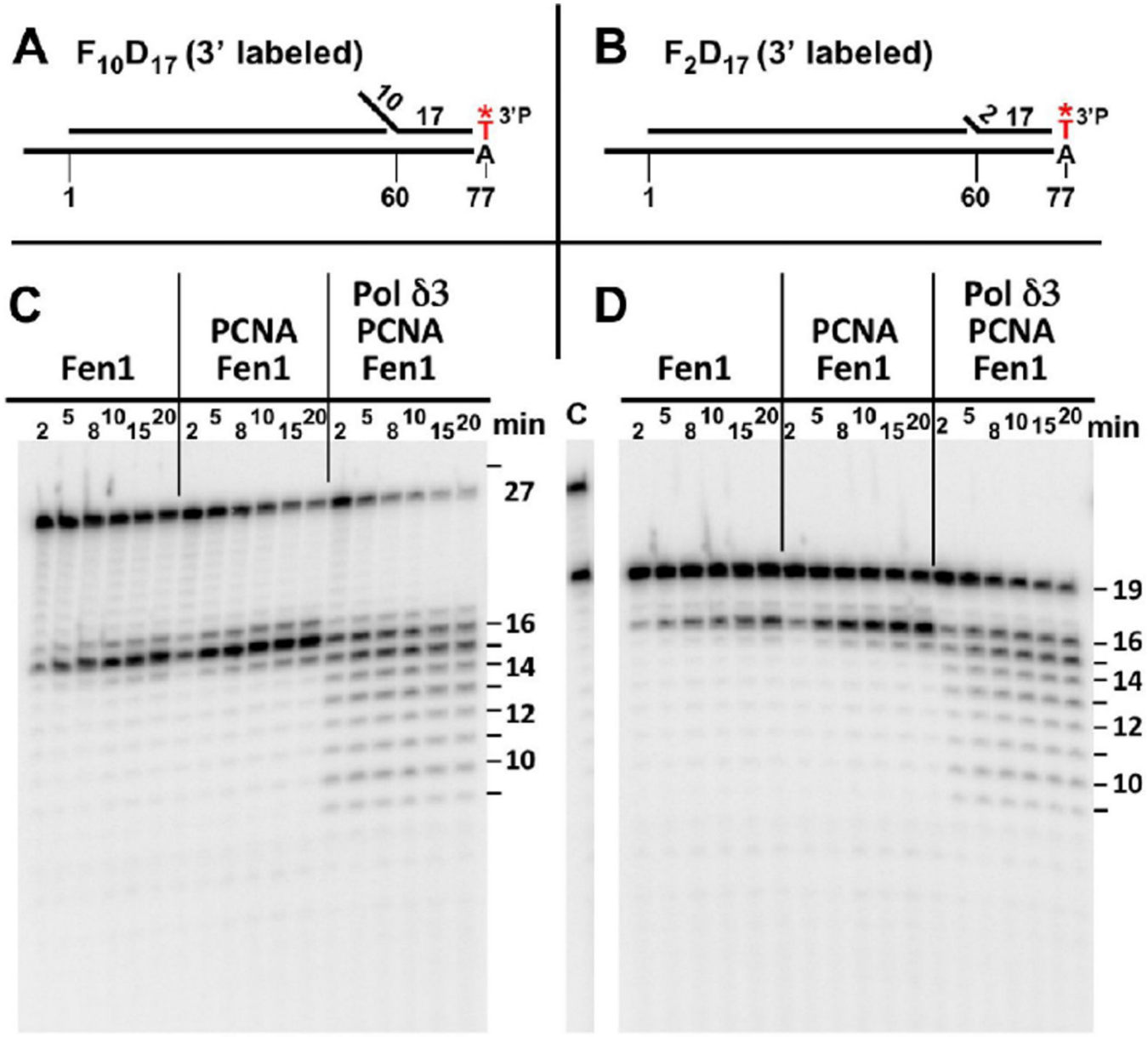

Figure 7. Cleavage of a 3'-[^{32}P]end labeled blocking oligonucleotide by Pol δ3 and Fen1

(A), (B) Diagram of the oligonucleotide substrates containing a 10 nt ($F_{10}D_{17}$) or a 2 nt (F_2D_{17}) flap at a nick. (C), (D) Product formation with the $F_{10}D_{17}$ and F_2D_{17} substrates, respectively. The substrates (20 nM) were incubated with 200 nM Fen1 in the presence or absence of 200 nM PCNA and 20 nM Pol δ3 at 37°C. The reactions were quenched at 2, 5, 8, 10, 15 and 20 min, analyzed by sequencing gel electrophoresis and visualized by phosphorimaging.

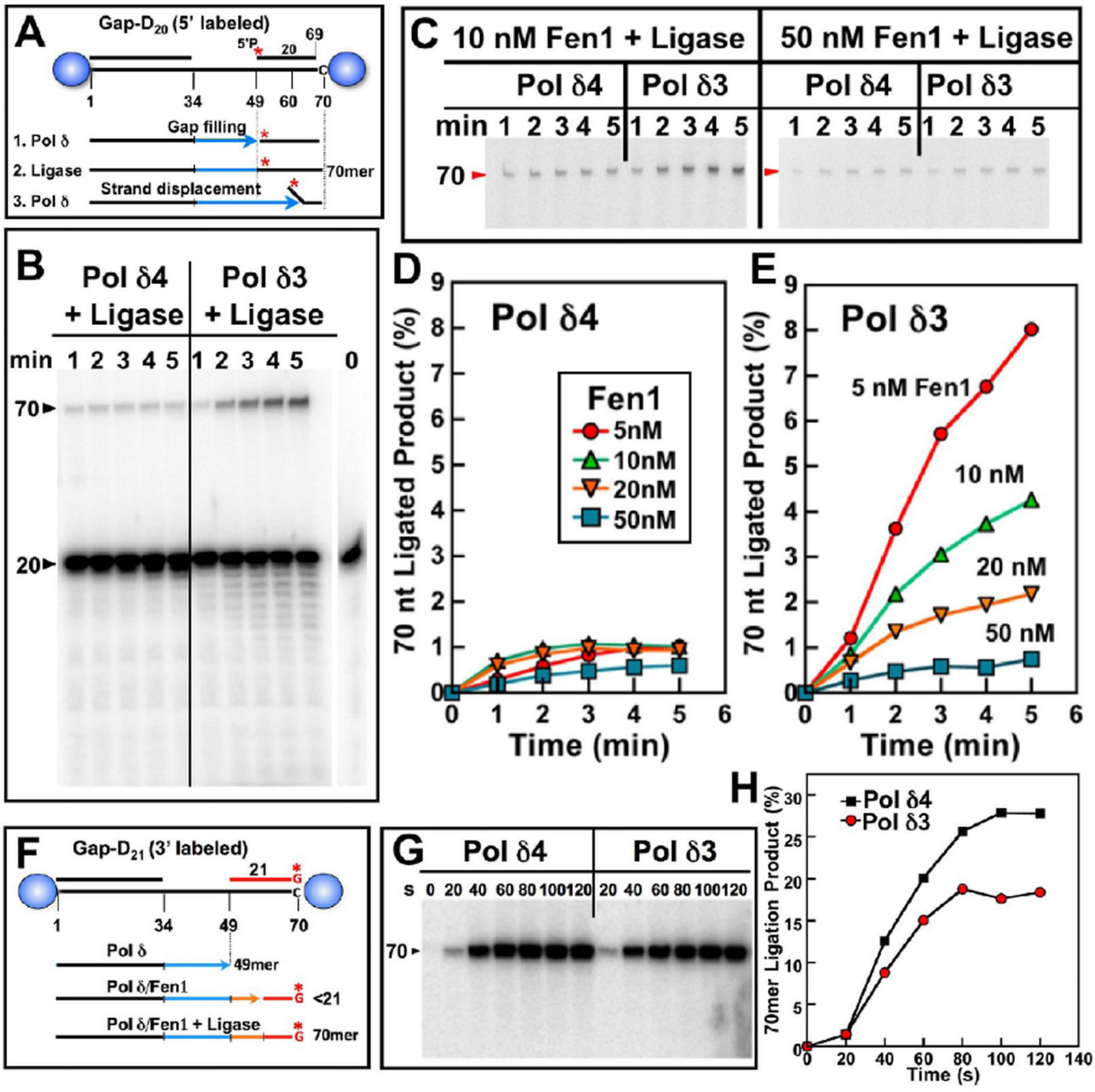

Figure 8. Ligation of primers extended by Pol δ4 and Pol δ3

(A) Diagram of the oligonucleotide substrate (Gap-D_{20}) for examination of the initial ligation step with Pol δ and DNA ligase I alone. (B) Comparison of the ligation products on the Gap-D_{20} substrate by Pol δ4 and Pol δ3. Gap-D_{20} (20 nM) was blocked with 50 nM streptavidin and then loaded with PCNA (40 nM) by 20 nM RFC. The reaction was initiated by addition of 5 nM DNA ligase I and 20 nM Pol δ4 or Pol δ3 at 37°C. The reactions were quenched at 1, 2, 3, 4 and 5 min. (C) Ligation in the complete system with Pol δ and Fen1. Reactions were performed as in B, and Fen1 was added at concentrations of 5, 10, 20 or 50 nM. Product formation was analyzed by gel electrophoresis and phosphorimaging. Gels for the 70mer product at the 10 and 50 nM Fen1 concentrations are shown. (D), (E) The 70mer

ligation product formation for the entire series in C was quantitated, and plotted against Fen1 concentration for Pol δ4 and Pol δ3, respectively. Data for Fen1 concentrations of 5, 10, 20, and 50 nM are shown as filled circles, triangles, inverted triangles and squares respectively. (F) Diagram of the 3'-[^{32}P]end labeled Gap-D_{21} substrate. (G). Reactions were performed as in C, with 100 nM Fen1, 20 nM Pol δ4 or Pol δ3, and 5 nM DNA ligase I. Reactions were quenched at 0, 20, 40, 60, 80, 100 and 120 sec, and analyzed by sequencing gels as before for the production of the 70mer ligation products. (H) The amounts of 70mer formed in G were quantitated and plotted against time for Pol δ4 (squares) and Pol δ3 (circles).

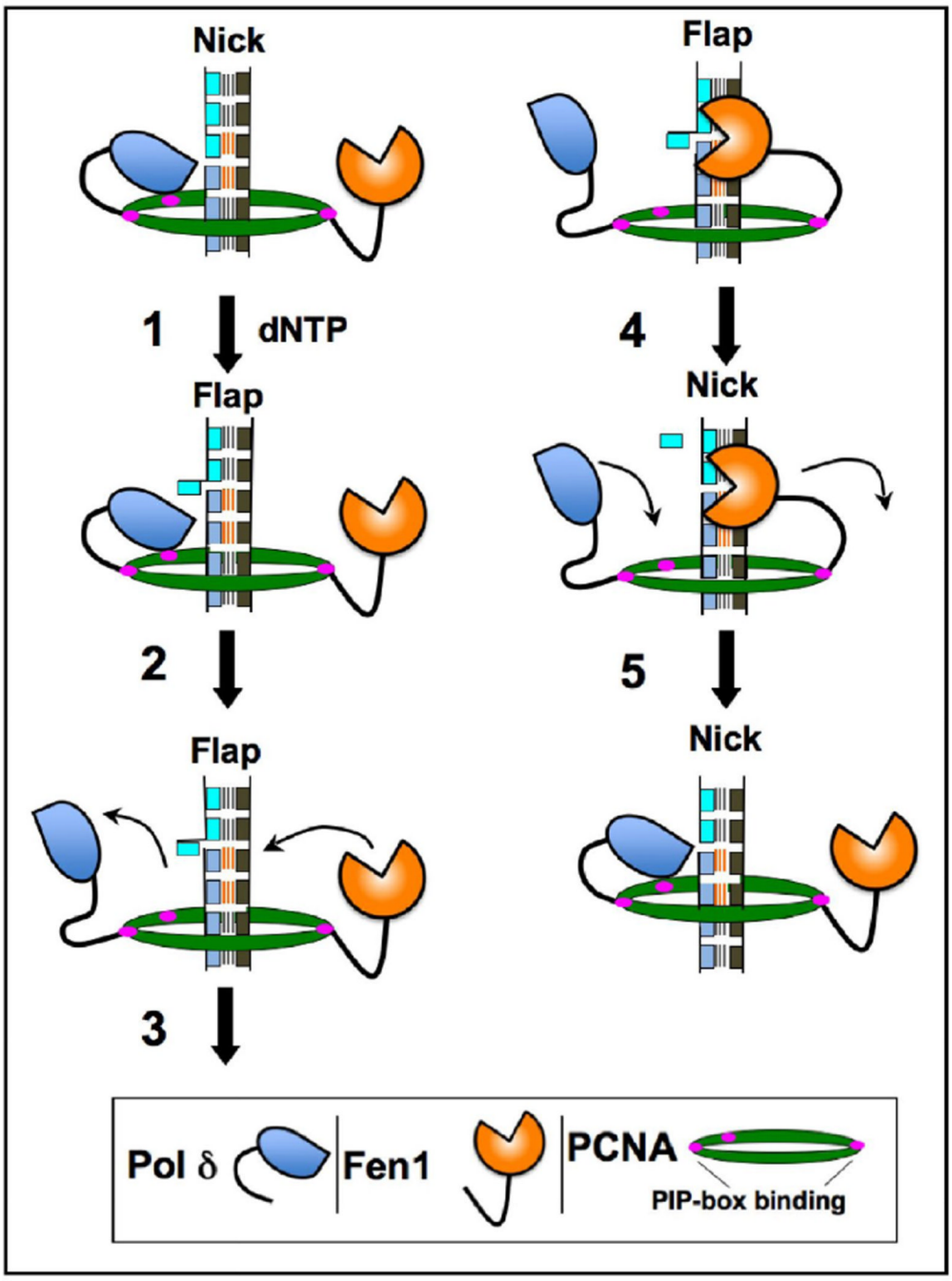

Fig. 9. Working model for the physical and functional coupling of Pol δ and Fen1 in the removal and replacement of the 5'-end of Okazaki fragments

The model depicts Pol δ and Fen1 simultaneously bound to PCNA. "1" Pol δ is shown having two contacts with PCNA, with Fen1 occupying the remaining PIP-box binding site. The DNA substrate is also shown as a nicked dsDNA, with Pol δ engaged with the DNA on the face of PCNA while Fen1 is in a conformation that is away from the face of PCNA. The series of transactions that are shown are based on the sequence shown in supplementary Fig. A1, "C", although essentially other arrangements with flaps of different sizes can be accommodated. The first reaction is the insertion of a single nucleotide by Pol δ, resulting in the formation of the a flap, generating the substrate for Fen1. "2" and "3" The formation of a

flap leads to the dissociation of Pol δ from the DNA, and the engagement of the flap structure by Fen1, essentially a switch between Pol δ and Fen1. “4” Fen1 cleaves the nick, generating a nick, which is the substrate for Pol δ. “5” The presence of the nick leads to a switch between Fen1 and Pol δ. This series of transactions is then repeated.